MEMORANDUM OF TRANSMITTAL

U.S. Army Research Office
ATTN: AMSRL-RO-BI (TR)
P.O. Box 12211
Research Triangle Park, NC 27709-2211

☒ Reprint (Orig + 2 copies)

☐ Technical Report (Orig + 2 copies)

☐ Manuscript (1 copy)

☐ Final Progress Report (Orig + 2 copies)

☐ Related Materials, Abstracts, Theses (1 copy)

CONTRACT/GRANT NUMBER: **W911NF0410224 (46637-CI-MUR)**

REPORT TITLE:

An explicit and unified error probability analysis of two detection schemes for differential unitary space-time modulation

SUBMITTED FOR PUBLICATION TO (applicable only if report is manuscript):

Thirty-Ninth Annual Asilomar Conference on Signals, Systems, and Computers
Pacific Grove, CA, Oct. 30 – Nov. 2, 2005

Sincerely,

Dr. James Zeidler
Department of Electrical and Computer Engineering
University of California, San Diego

REPORT DOCUMENTATION PAGE

Form Approved
OMB NO. 0704-0188

1. AGENCY USE ONLY (Leave Blank)

2. REPORT DATE
8/31/2005

3. REPORT TYPE AND DATES COVERED
Reprint: 01 June 2004 - 31 July 2005

4. TITLE AND SUBTITLE
An explicit and unified error probability analysis of two detection schemes for differential unitary space-time modulation

5. FUNDING NUMBERS
W911NF0410224

6. AUTHOR(S)
Haichang Sui, James R. Zeidler

7. PERFORMING ORGANIZATION NAME(S) AND ADDRESS(ES)
University of California - San Diego
Office of Contract & Grant Administration
9500 Gilman Dr. Mail Code 0934, La Jolla, CA, 92093-0934

8. PERFORMING ORGANIZATION REPORT NUMBER

9. SPONSORING / MONITORING AGENCY NAME(S) AND ADDRESS(ES)
U. S. Army Research Office
P.O. Box 12211
Research Triangle Park, NC 27709-2211

10. SPONSORING / MONITORING AGENCY REPORT NUMBER

11. SUPPLEMENTARY NOTES
The views, opinions and/or findings contained in this report are those of the author(s) and should not be construed as an official Department of the Army position, policy or decision, unless so designated by other documentation.

12 a. DISTRIBUTION / AVAILABILITY STATEMENT
Approved for public release; distribution unlimited.

12 b. DISTRIBUTION CODE
N/A

13. ABSTRACT (Maximum 200 words)

The performance of two detection schemes for the differential unitary space-time modulation (DUSTM), the standard detection and multiple-symbol decision-feedback detection, are analyzed in a unified approach under Rayleigh time-varying channels. We derive compact expressions for the pairwise error probability (PEP) and its upper and lower bound. Our formulas have both theoretical and computational advantages over existed ones. In particular, our analysis justifies the conventional design criteria on DUSTM constellations for more general channel models and detection schemes. We formulate a simple expression of the effective SNR that captures various effects such as the time correlation of fading, the number of received blocks used for symbol detection, and the noise variance. Based on the derived results for general DUSTMs, we further obtain explicit expressions of the PEP for the specific DUSTM proposed by Tarokh and Jafarkhani (2000). No numerical integration is needed to compute the PEP in this case. We also show that this specific DUSTM allow efficient multiple-symbol decision-feedback detection.

14. SUBJECT TERMS
N/A

15. NUMBER OF PAGES
5

16. PRICE CODE
N/A

17. SECURITY CLASSIFICATION OR REPORT	18. SECURITY CLASSIFICATION ON THIS PAGE	19. SECURITY CLASSIFICATION OF ABSTRACT	20. LIMITATION OF ABSTRACT
UNCLASSIFIED	**UNCLASSIFIED**	**UNCLASSIFIED**	**UL**

NSN 7540-01-280-5500

Standard Form 298 (Rev.2-89)
Prescribed by ANSI Std. 239-18
298-102

Enclosure 1

An Explicit and Unified Error Probability Analysis of Two Detection Schemes for Differential Unitary Space-Time Modulation

Haichang Sui and James R. Zeidler
Dept. of Electrical & Computer Engineering, Univ. of California, San Diego, La Jolla, CA 92093-0407
Emails: hsui@ucsd.edu, zeidler@ece.ucsd.edu

Abstract— **The performance of two demodulation schemes for the differential unitary space-time modulation (DUSTM), the standard differential demodulation and decision-feedback demodulation, are analyzed in a unified approach under Rayleigh time-varying channels. We derive compact expressions for the pairwise error probability (PEP) and its upper and lower bound. Our analysis justifies the conventional design criteria on DUSTM constellations for more general channel models and demodulation schemes. We formulate a simple expression of the effective SNR that captures the time correlation of fading, the length of the observation window, and the noise variance. Based on the derived results for general DUSTM, we further obtain an explicit closed-form expression of the PEP for the specific constellation proposed by Tarokh and Jafarkhani [12]. We also show that this specific DUSTM allow efficient decision-feedback detection.**

I. Introduction

Since it was first proposed in [1] and [2], differential unitary space-time modulation (DUSTM) has been proven to be an effective transmission scheme in fast-fading environment or scenario when reliable channel estimation is difficult to achieve. The DUSTM transmitter differentially encodes the space-time (ST) matrices to be transmitted. The redundancy embedded in the ST matrices provides diversity gain, while the memory in the received signal due to the time-correlation of the fading and the differential encoding is effectively exploited to noncoherently demodulate the transmitted symbols. For example, the previously received ST matrix is used as a reference for the currently received ST matrix in the *standard differential demodulation* (SDD) [1] [2]. It is shown in [1] that under certain assumptions, the effective SNR in SDD is 3dB less than the SNR when the channel is perfectly known. Such 3dB gap can be reduced by extending the observation window assumed in SDD, for example [4] [7] [8] [9] [10] [13], where the unknown information symbols are estimated either as a sequence or in a symbol-by-symbol manner.

In this paper, the pairwise error probability (PEP) and its upper/lower bounds are derived for the *decision-feedback demodulation* (DFD) of DUSTM signals when the fading channel is Rayleigh and time-invariant within the transmission of each ST matrix. As we will see later, SDD is a special case of the DFD and we can study the performance of both in a unified analysis. Similar expressions were derived in [1] for SDD under the Rayleigh *quasi-static* (QS) channel model where the channel is assumed to be constant for any two consecutive blocks. The results in [1] further motivate works such as [3] [5] [6] on DUSTM constellation design. For more general channel models and/or more advanced demodulation schemes such as MLSE and DFD [7] [8] [9] [10] [13], the resulting PEP expressions require computation of residues or infinite integrals from which it is hard to derive insightful bounds as in [1]. Consequently, this raises the question as to how DUSTM constellations should be designed for general channel models and detection schemes. The expressions derived in this paper have similar forms as their counterparts in [1], except that now the effective SNR not only depends on the noise variance but also on the time-correlation of the fading process and the length of the observation window. This suggests that the design criteria for DUSTM constellations proposed under SDD and QS channels remain valid for DFD and block-fading channels. Thus, the use of previously designed DUSTM constellations, including those in [3] [5] [6], is justified in more general scenarios. The notion of effective SNR is also presented in [11], where the authors consider SDD and assume a time-varying AR model for the channel. In contrast, our results apply for arbitrary block-fading channels and DFD. The performance of DFD under block-fading channels is also analyzed in [4] and [13]. However, [4] only addresses diagonal constellations and we show the upper bound on PEP in [13] is tight at high SNR by providing a new lower bound.

The PEP is derived here for general DUSTM constellations. Despite the fact that the resulting expression allows insightful bounds to be obtained, it still involves a finite integral which cannot be evaluated in closed-form. In this paper, it is further shown that this integral can be expressed into an explicit closed-form when the specific constellation proposed by Tarokh and Jafarkhani [12] is considered. We also show that the DFD for such a constellation can be implemented more efficiently than demodulating general DUSTM constellations. The low-complexity SDD proposed in [12] can be viewed as a special case of the DFD scheme implemented in Section V.

The rest of the paper is organized as follows. The system

This work is supported by, or in part by, the U. S. Army Research Office under the Multi-University Research Initiative (MURI) grant # W911NF-04-1-0224, the Office of Naval Research (Code 313), and the UCSD Center for Wireless Communications (UC IUCRP grant #03-10148)

model is presented in Section II. DFD is reviewed in Section III and its performance is analyzed in Section IV. Further analysis results and implementation of DFD are derived in Section V for the specific constellation in [12]. Section VI contains numerical results. Section VII concludes the paper.

II. System Model

The model for DUSTM in this paper is similar as in [1]. Denoting the number of transmit antenna to be M, a general DUSTM constellation $\mathcal{V}$ is defined as a set of $M \times M$ unitary matrices, that is,

$$\mathcal{V} = \{\mathbf{V}_0, \ldots, \mathbf{V}_{L-1}\} \ , \tag{1}$$

where L is the constellation size. Without loss of generality, we consider the transmission starting at time 0. The transmission is partitioned into blocks of time duration T_s. During the τth block $[\tau T_s, (\tau+1)T_s]$, $\log_2 L$ bits are mapped to $z_\tau \in \{0, \ldots, L-1\}$ and the corresponding matrix in $\mathcal{V}$ is differentially modulated as $\mathbf{S}_\tau = \mathbf{V}_{z_\tau}\mathbf{S}_{\tau-1}$, where $\mathbf{S}_{\tau-1}$ and $\mathbf{S}_\tau$ are the ST matrices transmitted in the previous block and the current block respectively. Symbols in the same row of $\mathbf{S}_\tau$ are transmitted at the same time from different antennas. The initial transmission $\mathbf{S}_0$ does not carry information and can be an arbitrary $M \times M$ unitary matrix. It is easy to see the data rate is $\frac{\log_2 L}{T_s}$ bits/second, if we ignore the initial transmission.

The channel is assumed to be Rayleigh fading, frequency-flat, and time-invariant in each T_s block. Consequently, we can collect the discrete channel gains in $[\tau T_s, (\tau+1)T_s]$ into a complex $M \times N$ matrix $\mathbf{H}_\tau$ where N is the number of receive antennas. We assume that the fading between different transmit-receive antenna pairs are i.i.d. zero-mean complex Gaussian processes. The time-correlation of the process $\{h_{\tau,m,n}\}_\tau$ is defined as $\varphi_{h,\xi} = E\left\{h_{\tau+\xi,i,j} \cdot h^*_{\tau,i,j}\right\}$ for $\xi = 0, \pm 1, \ldots$, where $h_{\tau,m,n}$ is the (m,n)th entry of $\mathbf{H}_\tau$.

As in [1], we can write the received ST signal in the τth block as an $M \times N$ complex matrix which is given by

$$\mathbf{R}_\tau = \mathbf{S}_\tau \mathbf{H}_\tau + \mathbf{W}_\tau \ . \tag{2}$$

Columns of $\mathbf{R}_\tau$ consist of symbols received on the corresponding antennas at different times within $[\tau T_s, (\tau+1)T_s]$. The $M \times N$ complex matrix $\mathbf{W}_\tau$ contains the additive noise at different receive antennas and different times. Entries in $\mathbf{W}_\tau$ are assumed to be i.i.d. $\mathcal{CN}(0, \sigma_w^2)$ random variables and uncorrelated in time. Without loss of generality, we normalize $\varphi_{h,0}$ to unity. By noticing the total transmit power is $\sum_{n=1}^{N} |\mathbf{S}_\tau(m,n)|^2 = 1$ at any time, it is easy to see that the received SNR on each antenna is $\rho = 1/\sigma_w^2$.

III. Decision-Feedback Demodulation

The DFD proposed in [4] [8] [9] [13] is reviewed in this section. We start from the likelihood function of receiving $\mathbf{R}_0, \ldots, \mathbf{R}_\tau$ given $z_1, \ldots, z_\tau$ are transmitted, that is,

$$f\left(\mathbf{R}_\tau^0 | z_\tau^1\right) = \det{}^{-N}(\pi \mathbf{C}_{r,\tau}) \exp\left\{-\mathrm{tr}\left[\left(\mathbf{R}_\tau^0\right)^H \mathbf{C}_{r,\tau}^{-1} \mathbf{R}_\tau^0\right]\right\}. \tag{3}$$

Here we use the notation $\mathbf{R}_\tau^0$ and z_τ^1 to denote $\left[\mathbf{R}_0^H, \ldots, \mathbf{R}_\tau^H\right]^H$ and $(z_1, \ldots, z_\tau)$, where the superscript $(\cdot)^H$ denotes matrix Hermitian. The matrix $\mathbf{C}_{r,\tau}$ in (3) is the covariance matrix of any column of the matrix $\mathbf{R}_\tau^0$. It can be shown that $\det^N(\pi \mathbf{C}_{r,\tau})$ does not depend on z_τ^1 and the exponent in $f\left(\mathbf{R}_\tau^0 | z_\tau^1\right)$ can be expressed as

$$\begin{aligned}\gamma_\tau\left(z_\tau^1\right) &\triangleq -\mathrm{tr}\left[\left(\mathbf{R}_\tau^0\right)^H \mathbf{C}_{r,\tau}^{-1} \mathbf{R}_\tau^0\right] \\ &= -\sum_{i=0}^{\tau} \frac{1}{\sigma_i^2} \left\| \left(\mathbf{\Lambda}_1^i\right)^H \mathbf{R}_i - \sum_{j=1}^{i} a_j^{(i)} \left(\mathbf{\Lambda}_1^{i-j}\right)^H \mathbf{R}_{i-j} \right\|^2\end{aligned} \tag{4}$$

where $\|\cdot\|$ denotes the matrix Frobenius norm and $\mathbf{\Lambda}_t^\tau \triangleq \mathbf{V}_{z_\tau} \cdot \mathbf{V}_{z_{\tau-1}} \cdots \mathbf{V}_{z_t}$ for $\tau \geq t$. The parameters $\{a_j^{(i)}\}_{j=1}^{i}$ are the optimal ith-order linear prediction coefficients of the process $\{h_{t,m,n} + w_{t,m,n}\}_t$ and σ_i is the associated linear prediction error variance. Furthermore, the cumulative log-likelihood metric $\gamma_\tau\left(z_\tau^1\right)$ can be expressed recursively as

$$\gamma_\tau\left(z_\tau^1\right) = \gamma_{\tau-1}\left(z_{\tau-1}^1\right) + \Delta_\tau\left(z_\tau; z_{\tau-1}^1\right) \ , \tag{5}$$

where

$$\Delta_\tau\left(z_\tau; z_{\tau-1}^1\right) = -\frac{1}{\sigma_\tau^2} \left\| \left(\mathbf{\Lambda}_1^\tau\right)^H \mathbf{R}_\tau - \sum_{j=1}^{\tau} a_j^{(\tau)} \left(\mathbf{\Lambda}_1^{\tau-j}\right)^H \mathbf{R}_{\tau-j} \right\|^2 \tag{6}$$

can be viewed as the branch metric for transition $z_{\tau-1}^1 \to z_\tau^1$. Unfortunately, the dependence of $\Delta_\tau\left(z_\tau; z_{\tau-1}^1\right)$ on the hypotheses of all previous transmitted symbols prevents efficient sequence estimation like the standard Viterbi algorithm. However, if we assume that the scalar processes $\{h_{t,m,n} + w_{t,m,n}\}_t$ can be modelled by a common AR(P) process, it can be shown that for $\tau \geq P$, (6) becomes

$$\begin{aligned}\Delta_\tau\left(z_\tau; z_{\tau-1}^1\right) &= -\frac{1}{\sigma_P^2} \left\| \mathbf{R}_\tau - \mathbf{V}_{z_\tau} \sum_{j=1}^{P} a_j^{(P)} \mathbf{\Lambda}_{\tau-j+1}^{\tau-1} \mathbf{R}_{\tau-j} \right\|^2 \\ &\triangleq \Delta_\tau\left(z_\tau; z_{\tau-1}^{\tau-P+1}\right) \quad .\end{aligned} \tag{7}$$

Thus, the branch metric in (7) only depends on $z_{\tau-1}^{\tau-P+1}$ instead of $z_{\tau-1}^1$ and the standard Viterbi algorithm can be applied. The linear prediction coefficients and prediction error can be solved from the Yule-Walker equations by

$$\begin{bmatrix} \varphi_{h,0} + \sigma_w^2 & \varphi_{h,-1} & \cdots & \varphi_{h,-P} \\ \varphi_{h,1} & \varphi_{h,0} + \sigma_w^2 & \cdots & \varphi_{h,-P+1} \\ \vdots & \vdots & \ddots & \vdots \\ \varphi_{h,P} & \cdots & \cdots & \varphi_{h,0} + \sigma_w^2 \end{bmatrix} \begin{bmatrix} -1 \\ a_1^{(P)} \\ \vdots \\ a_P^{(P)} \end{bmatrix} = \begin{bmatrix} -\sigma_P^2 \\ 0 \\ \vdots \\ 0 \end{bmatrix} . \tag{8}$$

The Viterbi algorithm has a complexity which is exponential in L since the number of states in the trellis is L^{P-1}. In order to further reduce the complexity, we consider a DFD scheme which has an approximate complexity of $O(L)$ per symbol. In DFD, $P-1$ previous decisions $\widehat{z}_{\tau-P+1}, \ldots, \widehat{z}_{\tau-1}$ are fed back and $P+1$ received blocks $\mathbf{R}_{\tau-P}, \ldots, \mathbf{R}_\tau$ are used to demodulate z_τ. Specifically, $z_{\tau-P+1}, \ldots, z_{\tau-1}$ in (7) are replaced by $\widehat{z}_{\tau-P+1}, \ldots, \widehat{z}_{\tau-1}$ and $\widehat{z}_\tau$ is demodulated as

$$\widehat{z}_\tau = \arg \max_{k=0,\ldots,L-1} \Delta_\tau\left(k; \widehat{z}_{\tau-1}^{\tau-P+1}\right) \ . \tag{9}$$

When $P=1$, the DFD requires no feedback and (9) reduces to the SDD in [7], which is an extension of the SDD in [1] and [2] to block-fading channels and the resulting z_τ is shown to maximize the likelihood function $f\left(\mathbf{R}_\tau^{\tau-1}|z_\tau\right)$. In the following section, the PEP for the DFD (9) will be derived by assuming perfect feedback. By setting $P=1$, the PEP for SDD can be easily obtained and the perfect feedback assumption becomes non-restrictive.

IV. Performance Analysis

A. PEP and its bounds

To facilitate deriving the PEP $P_e(k,l) \triangleq \Pr\{\hat{z}_\tau = k \mid z_\tau = l\}$, we consider a new test statistic which is equivalent to $\Delta_\tau\left(k;\hat{z}_{\tau-1}^{\tau-P+1}\right)$ in (9) for demodulation purpose. We assume the feedback decisions $\hat{z}_{\tau-1}^{\tau-P+1}$ are all correct in the following derivations. Some constants to be used later are defined as following.

$$\beta = 2\sqrt{\left(1+\sigma_w^2-\sigma_P^2\right)\left(1+\sigma_w^2\right)}, \quad \alpha = 1+\sigma_w^2-\frac{\beta}{2},$$
$$c=\sqrt{\beta/\left(\alpha+\beta\right)}, \quad \mu=\sqrt{\left(1+\sigma_w^2\right)/\left(1+\sigma_w^2-\sigma_P^2\right)}.$$

The new, equivalent test statistics can then be written as $Z_k = c^2||\boldsymbol{\Phi}_k^H\widetilde{\mathbf{R}}_\tau||^2$ where

$$\boldsymbol{\Phi}_k \triangleq \frac{1}{\sqrt{2}}\begin{bmatrix}\mathbf{I}_M\\ \mathbf{V}_k\end{bmatrix}, \quad \widetilde{\mathbf{R}}_\tau \triangleq \begin{bmatrix}\mu\mathbf{U}_\tau\\ \mathbf{R}_\tau\end{bmatrix}, \text{ and} \tag{10}$$

$$\mathbf{U}_\tau \triangleq \sum_{j=1}^{P} a_j^{(P)}\boldsymbol{\Lambda}_{\tau-j+1}^{\tau-1}\mathbf{R}_{\tau-j} \ . \tag{11}$$

It can be shown that the columns of $\widetilde{\mathbf{R}}_\tau$ are i.i.d. complex Gaussian vectors. Given that $z_\tau = l$, the covariance matrix of any column of $\widetilde{\mathbf{R}}_\tau$ is

$$\mathbf{C}_l = \beta\boldsymbol{\Phi}_l\boldsymbol{\Phi}_l^H + \alpha\mathbf{I}_{2M} \ . \tag{12}$$

The PEP is equal to the probability of $Z_k - Z_l > 0$ given $z_\tau = l$ is transmitted. To evaluate this probability, we first define the singular-value decomposition of $\boldsymbol{\Phi}_k^H\boldsymbol{\Phi}_l$ to be $\boldsymbol{\Theta}\mathbf{D}\boldsymbol{\Upsilon}^H$. Without loss of generality, we can assume $1 \geq d_{1,k,l} \geq \ldots \geq d_{M,k,l} \geq 0$ (see [14] pp.157, the upper bound 1 is from the fact that $\boldsymbol{\Phi}_l^H\boldsymbol{\Phi}_l = \mathbf{I}_M$). The singular values in $\mathbf{D} = \operatorname{diag}\left(d_{1,k,l},\ldots,d_{M,k,l}\right)$ are further related to the singular values of $\mathbf{V}_k - \mathbf{V}_l$ by

$$1-d_{m,k,l}^2 = \frac{1}{4}\sigma_m^2\left(\mathbf{V}_k-\mathbf{V}_l\right) \ . \tag{13}$$

After some algebra, $Z_k - Z_l$ can be reduced to

$$Z_k - Z_l = \sum_{n=1}^{N}\sum_{m=1}^{M}\mathbf{y}_{n,m}^H\mathbf{J}\mathbf{y}_{n,m} \ , \tag{14}$$

where $\mathbf{J} = \operatorname{diag}(-1,1)$. The 2×1 vectors $\{\mathbf{y}_{n,m}\}$ are zero-mean complex Gaussian and independent for different n or m. The covariance matrix of $\mathbf{y}_{n,m}$ is shown to be

$$\mathbf{C}_{y,m} = \begin{bmatrix}\beta & \beta d_{m,k,l}\\ \beta d_{m,k,l} & \frac{\beta}{\alpha+\beta}\left(\beta d_{m,k,l}^2+\alpha\right)\end{bmatrix} , \tag{15}$$

which is independent of n. Consequently, each summand in (14) is a quadratic form of complex Gaussian random vector $\mathbf{y}_{n,m}$ and its characteristic function can be written as

$$\begin{aligned}\phi_{m,k,l}(s) &= \mathrm{E}\left\{\exp\left(-s\cdot\mathbf{y}_{n,m}^H\mathbf{J}\mathbf{y}_{n,m}\right)\right\}\\ &= \det{}^{-1}\left(\mathbf{I}_2+s\mathbf{C}_{y,m}\mathbf{J}\right)\\ &= \left\{1+\bar{\rho}\sigma_{m,k,l}^2\left[\frac{1}{4}-\left(\alpha s+\frac{1}{2}\right)^2\right]\right\}^{-1}\end{aligned} \tag{16}$$

where $\sigma_{m,k,l}$ is the mth singular value of $\mathbf{V}_k - \mathbf{V}_l$ and

$$\bar{\rho} = \frac{\beta^2}{4\alpha\left(\alpha+\beta\right)} = \frac{1+\sigma_w^2}{\sigma_P^2}-1 \tag{17}$$

is defined as the effective SNR. By noticing the independence of $\mathbf{y}_{n,m}^H\mathbf{J}\mathbf{y}_{n,m}$ for different n or m, it is easy to see that the CF of $Z_k - Z_l$ is

$$\phi_{k,l}(s) = \prod_{m=1}^{M}\phi_{m,k,l}^N(s) \ , \tag{18}$$

Therefore, the PEP is given by

$$P_e(k,l) = \frac{1}{2\pi i}\int_0^\infty dz\int_{\mathcal{C}}\phi_{k,l}(s)\,e^{sz}ds \ , \tag{19}$$

By inspecting (16) and (18), it can be shown that the integral contour $\mathcal{C}: \operatorname{Re}(s) = -\frac{1}{2\alpha}$ guarantees the convergence of the integral in (19). The resulting PEP is

$$P_e(k,l) = \frac{1}{\pi}\int_0^{\pi/2}\prod_{m=1}^{M}\left[1+\frac{\bar{\rho}\sigma_{m,k,l}^2}{4\cos^2\theta}\right]^{-N}d\theta \ . \tag{20}$$

From (20), lower and upper bound on $P_e(k,l)$ can be easily obtained by noticing $\cos^2\theta \leq 1$. Specifically, the PEP is bounded by

$$C_2\prod_{m=1}^{M}\left(1+\frac{\bar{\rho}}{4}\sigma_{m,k,l}^2\right)^{-N} \leq P_e(k,l) \leq \frac{1}{2}\prod_{m=1}^{M}\left(1+\frac{\bar{\rho}}{4}\sigma_{m,k,l}^2\right)^{-N} \tag{21}$$

where $C_2 = \frac{1}{\pi}\int_0^{\pi/2}(\cos\theta)^{2MN}d\theta$.

B. Constellation design considerations

An upper bound similar to (21) was derived in [1] (see also (8) in [3] or (7) in [5]) for SDD under the QS channel model, which motivates various design criteria for DUSTM constellations based on maximizing the so-called *diversity-product* $\zeta \triangleq \frac{1}{2}\min_{k\neq l}\left[\prod_m \sigma_{m,k,l}\right]^{1/M}$ [1] [3] [5] or the so-called *diversity-sum* $\xi \triangleq \frac{1}{2\sqrt{M}}\min_{k\neq l}\left[\sum_{m=1}^M \sigma_{m,k,l}^2\right]^{1/2}$ [5]. In this paper, a lower bound is presented in (21). It can be seen from (21) that these design criteria are still valid when DFD is used instead of SDD and/or the channel is block-fading instead of QS, since

$$\max_{k\neq l}\prod_{m=1}^{M}\left(1+\frac{\bar{\rho}}{4}\sigma_{m,k,l}^2\right)^{-N} \approx \begin{cases}\frac{1}{2}\left[1+M\bar{\rho}\xi^2\right]^{-N} & \text{when } \bar{\rho} \ll 1\\ \frac{1}{2}\left(\bar{\rho}\zeta^{-2}\right)^{-MN} & \text{when } \bar{\rho} \gg 1\end{cases} . \tag{22}$$

Consequently, constellations maximizing ζ or ξ will be optimal in high or low SNR range, respectively.

C. Effective SNR

We have defined the effective SNR $\overline{\rho}$ in (17), which depends not only on the AWGN power σ_w^2 but also on the time correlation of the fading process and the observation window length P. It is easy to see that $\overline{\rho} \leq \rho$ since the AWGN is uncorrelated in time and $\sigma_P^2 \geq \sigma_w^2$ for arbitrary P. Interestingly, $\overline{\rho} = \rho^2 / (2\rho + 1)$ when $P = 1$ and $\varphi_{h,1} = 1$, which is consistent with the results derived for SDD under QS assumption in [1] [3] [5]. The well-known 3dB gap between SDD and coherent demodulation can be seen from $\overline{\rho} \approx \rho/2$ when $\rho \gg 1$, as ρ has been shown to be the SNR for coherent demodulation in [1] [13]. When the QS assumption is not satisfied, i.e. $|\varphi_{h,1}| < 1$, the effective SNR for SDD becomes

$$\overline{\rho} = \frac{|\varphi_{h,1}|^2 \rho^2}{\left(1 - |\varphi_{h,1}|^2\right) \rho^2 + 2\rho + 1} ,$$

which converges to a finite value $|\varphi_{h,1}|^2 / \left(1 - |\varphi_{h,1}|^2\right)$ as $\rho \to \infty$. For general block-fading channels, the effective SNR is bounded even if $\rho = \infty$, which is the well-known "error-floor" effect. The error-floor can be reduced by increasing P, although this may lead to more error propagation as well.

V. Results for DUSTM in [12]

The results derived in the previous section apply for general DUSTM. Although the PEP expression (20) allows insightful bounds to be obtained, it still involves a finite integral which cannot be evaluated in closed-form. In this section, we focus on a class of special DUSTM constellations proposed in [12] for two transmit antennas. Such constellations are specified as follows. The size of the constellation L is equal to 2^{2b} for some positive integer b. The matrix $\mathbf{V}_l \in \mathcal{V}$ $(l = 0, \ldots, L-1)$ is given by

$$\mathbf{V}_l = \frac{1}{2} \begin{bmatrix} x_l + y_l & -x_l + y_l \\ x_l^* - y_l^* & x_l^* + y_l^* \end{bmatrix} , \tag{23}$$

where x_l, y_l are 2^b-PSK symbols. It is noticed that $\mathbf{V}_l$ is Hamiltonian [3]. In addition, entries in each $\mathbf{V}_l$ have interesting structures. As we will see later, the integral in (20) can be evaluated in closed-form and efficient implementation of the DFD is available by exploiting these properties.

Specifically, the singular values of any 2×2 Hamiltonian matrix can be shown to coincide. By further examining the structure in the entries of $\mathbf{V}_l$, the singular value of $\mathbf{V}_k - \mathbf{V}_l$ with double duplicity is given by

$$\sigma_{k,l} = \sqrt{2 - \mathrm{Re}\left(x_k x_l^*\right) - \mathrm{Re}\left(y_k y_l^*\right)} \tag{24}$$

and $\sigma_{k,l} = 0$ iff $k = l$. Thus, the CF of $Z_k - Z_l$ in (18) becomes

$$\phi_{k,l}(s) = \left\{ 1 + \overline{\rho}\sigma_{k,l} \left[\frac{1}{4} - \left(\alpha s + \frac{1}{2} \right)^2 \right] \right\}^{-2N} . \tag{25}$$

By taking the inverse Laplace transform of $\phi_{k,l}(s)$, the probability density function of $Z_k - Z_l$ is shown to be

$$f_{k,l}(x) = \frac{1}{a_{k,l}} \exp\left(-\frac{b_{k,l}}{a_{k,l}} |x| - \frac{x}{2\alpha} \right) \sum_{n=1}^{2N} \frac{g_{n,k,l} |x|^{n-1}}{a_{k,l}^{n-1} (n-1)!} \tag{26}$$

where

$$b_{k,l} = \sqrt{1 + \overline{\rho}\sigma_{k,l}^2 / 4} , \tag{27}$$

$$a_{k,l} = \alpha \sigma_{k,l} \sqrt{\overline{\rho}} , \tag{28}$$

$$g_{n,k,l} = \binom{4N - n - 1}{2N - 1} (2 b_{k,l})^{-4N+n} . \tag{29}$$

Thus, $P_e(k,l)$ can be expressed in closed-form as

$$P_e(k,l) = \int_0^\infty f_{k,l}(x)\, dx = \sum_{n=1}^{2N} g_{n,k,l} \left(b_{k,l} + \frac{a_{k,l}}{2\alpha} \right)^{-n} . \tag{30}$$

An important advantage of the DUSTM constellations in [12] is that they allow efficient ML demodulation for SDD. In the following, we show that the complexity of DFD for such constellations can also be reduced similarly to their SDD. Substituting (23) into $\Delta_\tau \left(k; \widehat{z}_{\tau-1}^{\tau-P+1}\right)$ in (9) and after some algebra, the test statistic reduces to

$$\Delta_\tau \left(k; \widehat{z}_{\tau-1}^{\tau-P+1}\right) = -\frac{1}{2\sigma_P^2} \left[|x_k - \overline{v}_{x,\tau}|^2 + |y_k - \overline{v}_{y,\tau}|^2 \right] + c \tag{31}$$

where the term c only depends on $z_{\tau-1}^{\tau-P+1}$ and $\mathbf{R}_\tau^{\tau-P}$ but not on k. If we define $\overline{\mathbf{U}}_\tau$ similar as $\mathbf{U}_\tau$ except using the feedback decisions $\widehat{z}_{\tau-1}^{\tau-P+1}$ in (11), the quantities $\overline{v}_{x,\tau}$ and $\overline{v}_{y,\tau}$ in (31) can be given by

$$\begin{bmatrix} \overline{v}_{x,\tau} \\ \overline{v}_{y,\tau} \end{bmatrix} = \begin{bmatrix} 1 & 1 \\ 1 & -1 \end{bmatrix} \begin{bmatrix} \overline{\mathbf{u}}_{\tau,2} \mathbf{r}_{\tau,2}^H + \mathbf{r}_{\tau,1} \overline{\mathbf{u}}_{\tau,1}^H \\ \overline{\mathbf{u}}_{\tau,1} \mathbf{r}_{\tau,2}^H - \mathbf{r}_{\tau,1} \overline{\mathbf{u}}_{\tau,2}^H \end{bmatrix} \tag{32}$$

where $\mathbf{r}_{\tau,1}$, $\mathbf{r}_{\tau,2}$ and $\overline{\mathbf{u}}_{\tau,1}$, $\overline{\mathbf{u}}_{\tau,2}$ are $1 \times N$ row vectors of $\mathbf{R}_\tau$ and $\overline{\mathbf{U}}_\tau$ respectively. That is,

$$\mathbf{R}_\tau = \begin{bmatrix} \mathbf{r}_{\tau,1} \\ \mathbf{r}_{\tau,2} \end{bmatrix}, \quad \overline{\mathbf{U}}_\tau = \begin{bmatrix} \overline{\mathbf{u}}_{\tau,1} \\ \overline{\mathbf{u}}_{\tau,2} \end{bmatrix} .$$

By observing (31), it is noticed that demodulation for the constellations in [12] is equivalent to find the closest point to $\overline{v}_{x,\tau}$ and $\overline{v}_{y,\tau}$ in a $\sqrt{L}$-PSK constellation separately. In contrast, demodulating z_τ for a general DUSTM constellation involves L matrix multiplications to obtain $\mathbf{V}_k^H \mathbf{R}_\tau$ in (7) for $k = 0, \ldots, L-1$. Therefore, the complexity of DFD is lower for the constellations in [12] than general 2×2 DUSTM constellations, if we ignore the additional computation in forming (32) and mapping from (x_k, y_k) to k.

VI. Numerical Results

In this section, numerical results are presented to verify the analysis and obtain insights on how the time-variation of the channel and the choice of P affect the performance. The MIMO channel is generated by Jakes' model as a number of i.i.d. complex Gaussian random processes. The number of transmit antennas is chosen to be 2, so is the number of receive antennas. The constellation proposed in [12] is used with the constellation size $L = 16$.

In Fig.1, the simulated symbol error probabilities (markers) are plotted against the analytic symbol error probabilities (curves) with the normalized Doppler frequency $f_d T_s$ set to 0.05. The analytic values are obtained from (30) and the union bound, that is,

$$P_e \approx \frac{1}{L} \sum_{l=0}^{L-1} \sum_{k=0, k \neq l}^{L-1} P_e(k,l) \ . \qquad (33)$$

We notice that in Fig.1 the analytic and simulated values are close for different values of P and/or received SNR ρ. Recalling that perfect feedback is assumed in analyzing the PEP, Fig.1 shows that the error propagation is not severe and the union bound is accurate at a wide range of P and/or ρ for this constellation.

To better understand the effect of time-variation of the channel and the choice of P, the effective SNR $\overline{\rho}$ versus ρ and $f_d T_s$ are plotted in Fig.2(a) and Fig.2(b), respectively. The accuracy of using $\overline{\rho}$ in characterizing the demodulation performance has been verified in Fig.1. The normalized Doppler frequency in Fig.2(a) is fixed to 0.05 while the received SNR is set to 24dB in Fig.2(b). An error floor is observed at high SNR for SDD ($P = 1$) but not for DFD with $P = 5, 9$ in Fig.2(a). We can also see from Fig.2(b) that $\overline{\rho}$ of SDD decreases more rapidly than DFD as the time-variation of the channel increases. The gap in the effective SNR between DFD and SDD is significant when either ρ or $f_d T_s$ is large.

VII. Conclusion

The pairwise error probability and its upper/lower bounds are derived in this paper for DFD of DUSTM signals when the channel is Rayleigh block-fading. The analysis also apply for SDD, which is a special case of DFD. Our results show that the design criteria derived for SDD and quasi-static channel model remain valid when DFD is used and the channel varies between consecutive blocks. The time-variation of the channel and the length of the observation window in DFD determine the effective SNR, which is given in a compact expression. For the specific DUSTM constellation in [12], closed-form expression for the PEP is derived and an efficient implementation of the DFD is presented. The analysis is verified by numerical results and significant gain due to DFD is observed at high SNR or high time-variation of the channel.

References

[1] B. M. Hochwald, W. Sweldens, "Differential unitary space-time modulation", *IEEE Trans. Comm.*, Dec. 2000

[2] B. L. Hughes, Differential space-time modulation, IEEE Trans. Info. Theory, Nov. 2000

[3] A. Shokrollahi,et al, "Representation theory for high-rate multiple antenna code design", *IEEE Trans. I.T.*, Sept. 2001

[4] R. Schober, L. H.-J. Lampe, "Noncoherent receivers for differential space-time modulation", *IEEE Trans. Comm.*, May 2002

[5] X.-B. Liang, X.-G. Xia, "Unitary signal constellations for differential space-time modulation with two transmit antennas: parametric codes, optimal designs, and bounds", *IEEE Trans. I.T.*, Aug. 2002

[6] B. L. Hughes, "Optimal space-time constellations from groups", *IEEE Trans. I.T.*, Feb. 2003

[7] E. Chiavaccini, G. M. Vitetta, "Further results on differential space-time modulation", *IEEE Trans. Comm.*, July 2003

[8] C. Ling, et al, "Multisampling decision-feedback linear prediction receivers for differential space-time modulation over Rayleigh fast-fading channels", *IEEE Trans. Comm.*, July 2003

[9] C. Ling, et al, "On decision-feedback detection of differential space-time modulation in continuous fading", *IEEE Trans. Comm.*, Oct. 2004

[10] P. Tarasak, et al, "Improved approximate maximum-likelihood receiver for differential space-time block codes over Rayleigh-fading channels", *IEEE Trans. Veh. Tech.*, Mar. 2004

[11] C. B. Peel, A. L. Swindlehurst, "Performance of space-time modulation for a generalized time-varying Rician channel model", *IEEE Trans. Wireless Comm.*, May 2004

[12] V. Tarokh, H. Jafarkhani, "A differential detection scheme for transmit diversity", *IEEE J. Sel. Areas in Comm.*, July 2000

[13] B. Bhukania, P. Schniter, "On the robustness of decision-feedback detection of DPSK and differential unitary space-time modulation in Rayleigh-fading channels", *IEEE Trans. Wireless Comm.*, Sept. 2004

[14] R. A. Horn, C. R. Johnson, Matrix Analysis, Cambridge University Press, Cambridge, 1995

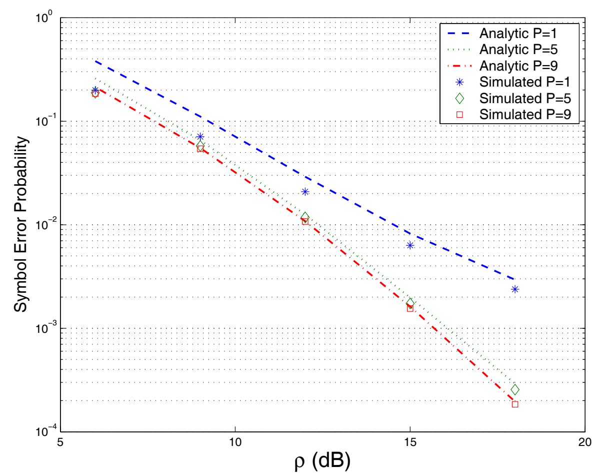

Fig. 1. Analytic and simulated symbol error probability

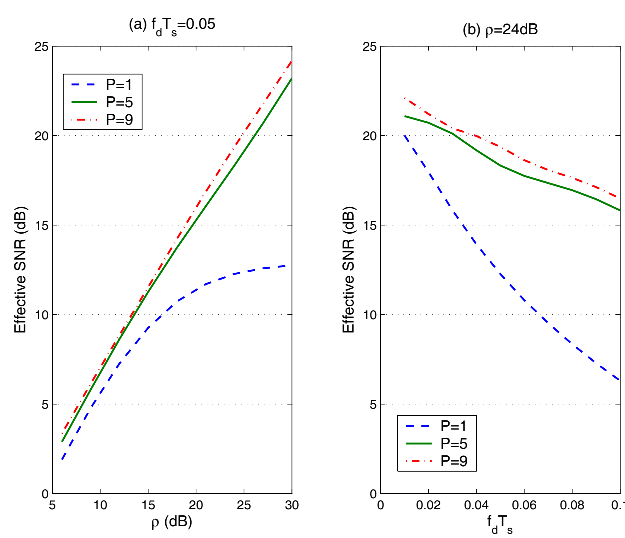

Fig. 2. Effective SNR versus received SNR ρ